iScience

CellPress
OPEN ACCESS

Article

Noncanonical protease-activated receptor 1 regulates lymphatic differentiation in zebrafish

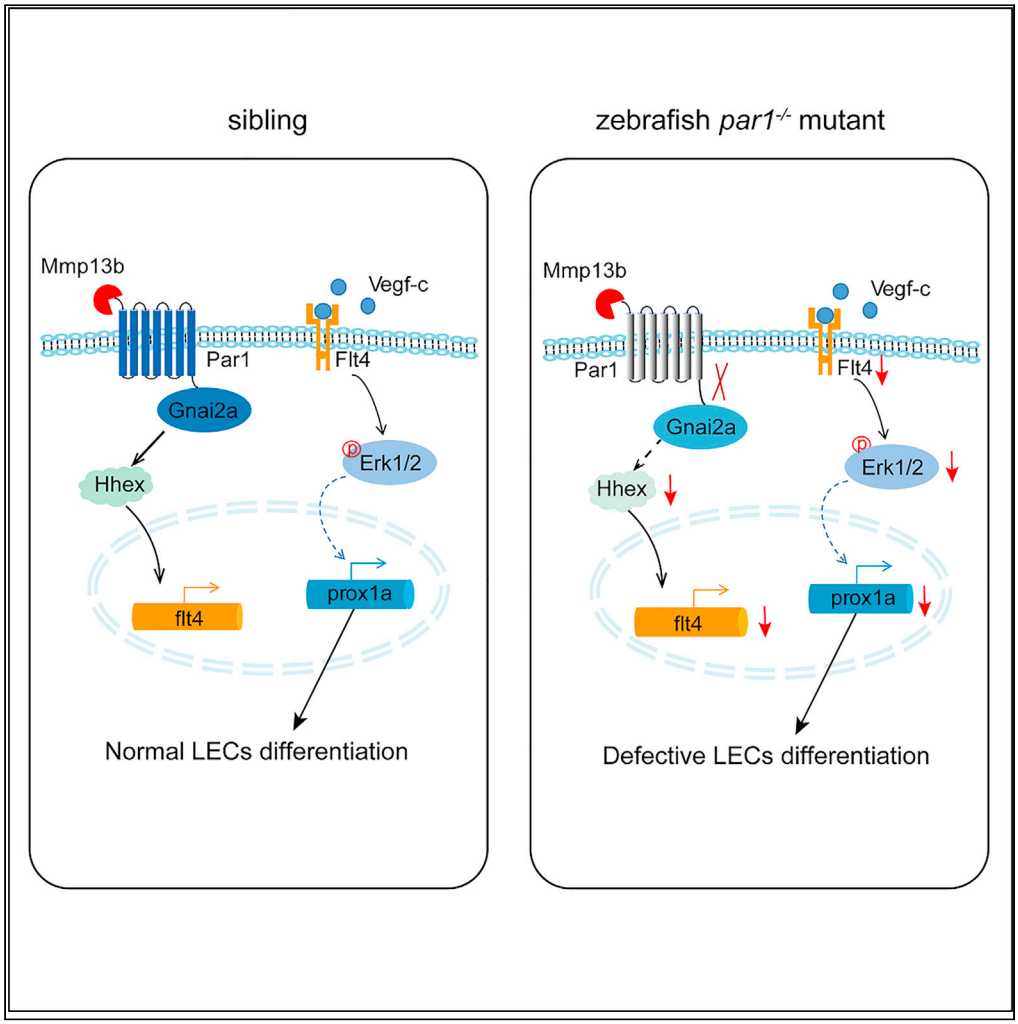

Daoxi Lei, Xiuru Zhang, Muhammad Abdul Rouf, ..., Tao Zhang, Guixue Wang, Yeqi Wang

wanggx@cqu.edu.cn (G.W.)
yeqi.wang@cqu.edu.cn (Y.W.)

Highlights

The Mmp13b-Par1-Gnai2a axis regulates lymphatic differentiation in zebrafish

Par1 mutant showed decreased prox1a expression in parachordal lymphangioblasts

Par1 promotes *flt4* expression in the posterior cardinal vein of zebrafish embryos

Lei et al., iScience *24*, 103386
November 19, 2021
https://doi.org/10.1016/j.isci.2021.103386

iScience

CellPress
OPEN ACCESS

Article

Noncanonical protease-activated receptor 1 regulates lymphatic differentiation in zebrafish

Daoxi Lei,[1,2,4] Xiuru Zhang,[1,4] Muhammad Abdul Rouf,[1,4] Yoga Mahendra,[1] Lin Wen,[1] Yan Li,[1] Xiaojuan Zhang,[1] Li Li,[3] Luming Wang,[1] Tao Zhang,[1] Guixue Wang,[1,*] and Yeqi Wang[1,5,*]

SUMMARY

The differentiation of lymphatic progenitors is a crucial step in lymphangiogenesis. However, its underlying mechanism remains unclear. Here, we found that noncanonical protease-activated receptor 1 (*par1*) regulates the differentiation of lymphatic progenitors in zebrafish embryos. Loss of *par1* function impaired lymphatic differentiation by downregulating *prox1a* expression in parachordal lymphangioblasts and caused compromised thoracic duct formation in zebrafish. Meanwhile, the G protein *gnai2a*, a *par1* downstream effector, was selectively required for lymphatic development in zebrafish, and its mutation mimicked the lymphatic phenotype observed in *par1* mutants. Interestingly, mmp13, but not thrombin, was required for lymphatic development in zebrafish. Furthermore, analyses of genetic interactions confirmed that *mmp13b* serves as a *par1* upstream protease to regulate lymphatic development in zebrafish embryos. Mechanistically, *par1* promotes *flt4* expression and phospho-Erk1/2 activity in the posterior cardinal vein. Taken together, our findings highlight a function of *par1* in the regulation of lymphatic differentiation in zebrafish embryos.

INTRODUCTION

The lymphatic system is a complex vasculature that originates from a preexisting embryonic vein. It has crucial functions in maintaining the interstitial fluid balance and retrieving water and macromolecules, taking up lipids, and also providing the major conduit for immune cells to take part in the immune surveillance system (Alitalo, 2011). Malformation of the lymphatic system can lead to many pathologies, such as tissue fluid accumulation, edema or lymphedema, cancer cell dissemination, and inflammation (Schulte-Merker et al., 2011).

During the development of the lymphatic system of mice, a sub-population of venous endothelial cells (VECs) expresses the transcription factor prospero homeobox protein 1 (PROX1) and differentiates into lymphatic progenitors in the cardinal vein (CV) at embryonic day 9.5 (E9.5) (Wigle et al., 2002; Wigle and Oliver, 1999). Ablation of *prox1* in mice prevents the development of lymphatic vessels, and the ectopic expression of *prox1* in endothelial cells (ECs) of blood vasculature upregulates lymphatic endothelial cell (LEC) markers (Kim et al., 2010; Wigle and Oliver, 1999). These studies suggest that *prox1* is both necessary and sufficient to induce LEC fate (Hong et al., 2002; Wigle et al., 2002). In zebrafish embryos, lymphatic progenitors are induced within the ventral posterior cardinal vein (PCV) at an early stage, approximately 26 h postfertilization (hpf) (Nicenboim et al., 2015). The LECs show *prox1a* expression and move away to vacate the PCV in response to the sprouting process (Koltowska et al., 2015). These lymphatic progenitors migrate to the horizontal myoseptum (HM) region to form parachordal lymphangioblasts (PLs), a pool of lymphatic precursor cells, at about 48 hpf. Afterward, the PLs migrate in two directions, ventrally to form the thoracic duct (TD) and dorsally to form the dorsal longitudinal lymphatic vessel (DLLV); this is completed at around 5 days postfertilization (dpf) (Cha et al., 2012). Maternal and zygotic *prox1a* mutant leads to defective lymphatic development in zebrafish embryos, indicating its conserved role in the lymphatic vasculature. Recent studies have shown that a crucial role of Vegfc-Flt4 and its downstream effector Erk1/2 involves the induction of *prox1a* expression and LEC sprouting in zebrafish trunk (Koltowska et al., 2015; Shin et al., 2016).

[1]Key Laboratory for Biorheological Science and Technology of Ministry of Education, State and Local Joint Engineering Laboratory for Vascular Implants, Bioengineering College of Chongqing University, Chongqing 400030, China

[2]Department of Ophthalmology, Chongqing Hospital of Traditional Chinese Medicine, Chongqing 400021, China

[3]School of Life Science and Technology, Harbin Institute of Technology, Harbin 150080, China

[4]These authors contributed equally

[5]Lead contact

*Correspondence: wanggx@cqu.edu.cn (G.W.), yeqi.wang@cqu.edu.cn (Y.W.)

https://doi.org/10.1016/j.isci.2021.103386

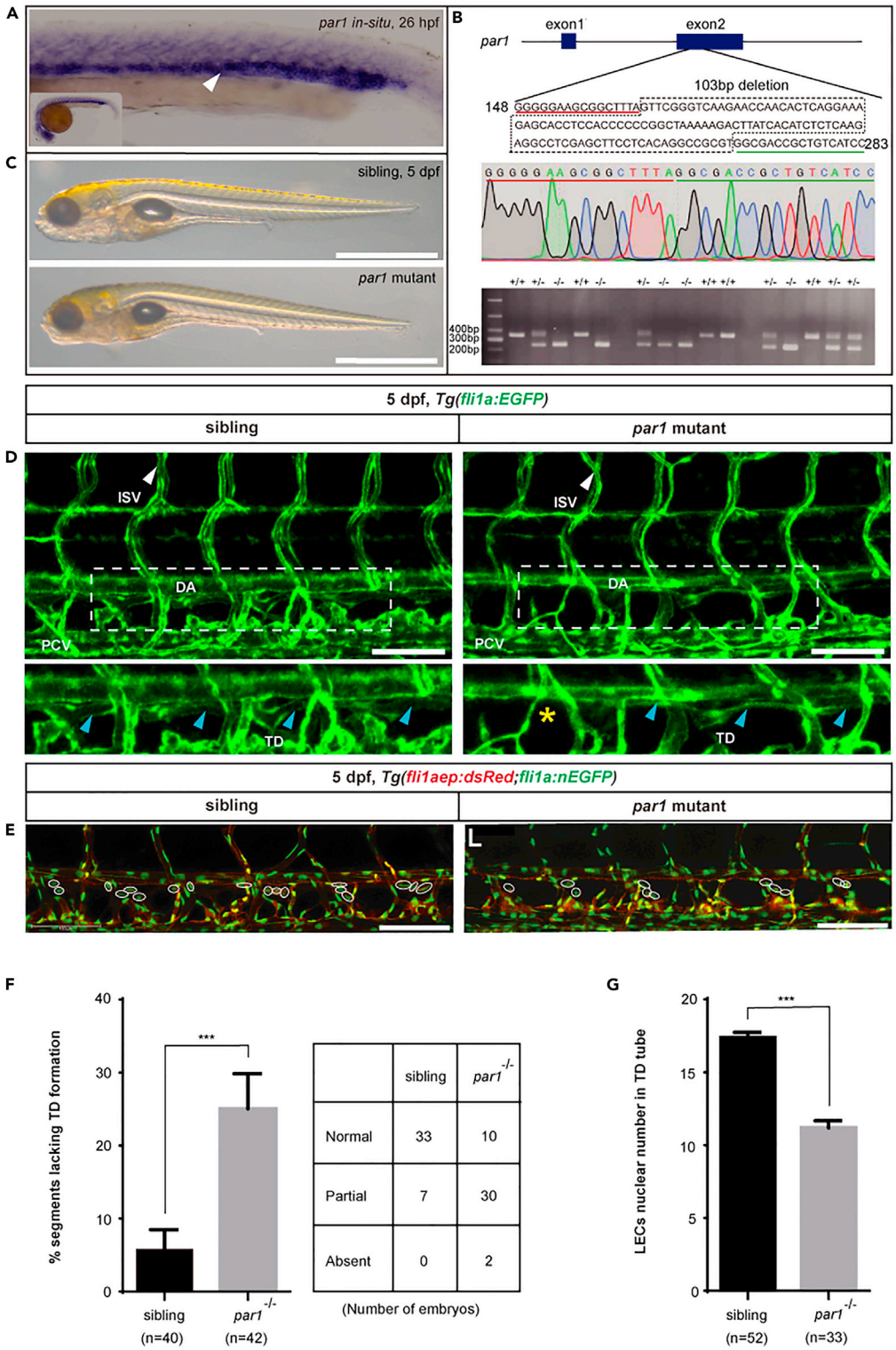

	sibling	par1 -/-
Normal	33	10
Partial	7	30
Absent	0	2

Figure 1. *par1* mutant zebrafish embryos show defective TD formation

(A) WISH of *par1* gene expression in zebrafish embryos at 26 hpf. The white arrowhead indicates the expression of the *par1* gene in the PCV.

(B) Brightfield lateral views of sibling and *par1* homozygous mutant zebrafish embryos at 5 dpf. Scale bars: 1 mm.

Figure 1. *Continued*

(C) Top row, schematic representation of the generated *par1* zebrafish mutant; middle, results of sequencing for validating *par1* mutants; bottom, DNA gel results for genotyping wildtype (+/+), heterozygous (+/−), and homozygous mutant (−/−) embryos.

(D) Confocal images showing TD formation of sibling and *par1* homozygous mutants using the *Tg(fli1a:EGFP)* line at 5 dpf. Blue arrowheads indicate the presence of TD formation in each somite; yellow asterisks represent the absence of TD formation in each somite; DA and PCV areas are denoted. Scale bars: 100 μm.

(E) Confocal images showing the nuclear numbers of LECs in the TD tube in *Tg(fli1aep:dsRed;fli1:nEGFP)* siblings and *par1* zebrafish mutants at 5 dpf. White circles indicate the presence of LECs nuclear numbers in the TD tube. Scale bars: 100 μm.

(F) Percentage of somites lacking TDs in siblings (n = 40 embryos) and *par1* homozygous mutants (n = 42 embryos); 6 somites/embryos were used for quantification. Right is the table showing the number of embryos with normal TD, partial TD, and without TD, respectively.

(G) LECs nuclear number in the TD tube of siblings (n = 52 embryos) and *par1* homozygous mutants (n = 33 embryos); 6 somites/embryos were used for quantification. In (F) and (G), values represent means ± SEMs. *$p \leq 0.001$ in the Student's t test. See also Figure S1.

Protease-activated receptor 1 (PAR1) is a G-protein-coupled receptor (GPCR), more specifically, a thrombin receptor (F2r) that plays a critical role in vascular biology (Alberelli and De Candia, 2014; Coughlin, 2005). It is activated through cleavage of the N-terminal exodomain by the serine protease thrombin (F2) at a canonical site (Vu et al., 1991). However, other PAR1 upstream proteases have been found to activate PAR1 (Alberelli and De Candia, 2014). For example, matrix metalloproteases (MMPs), especially MMP1 and MMP13, can also cleave and activate PAR1 at a noncanonical site, which leads to a signaling pattern that is distinct from that seen with F2 (Austin et al., 2013; Galt et al., 2002; Jaffré et al., 2012; Trivedi et al., 2009). Once irreversibly cleaved and activated by different proteases at either canonical or noncanonical sites, PAR1 can couple to and activate multiple heterotrimeric G protein subtypes including $G_{12/13}$, $G_{11/q}$, and G_i . This results in a multitude of cellular signaling events including the activation of MAPK/ERK signaling (Soh et al., 2010; Zhao et al., 2014). Par1 has been reported to play a pivotal role in hematopoiesis (Yue et al., 2012) and cardiovascular development in zebrafish (Ellertsdottir et al., 2012). Although *par1* is enriched in the PCV of zebrafish embryos at 1 dpf (Xu et al., 2011), its role within it remains unknown.

Here, we report that the Mmp13b-Par1-Gnai2a axis regulates the differentiation of lymphatic progenitors in zebrafish embryos. Mechanistically, we show that *par1* promotes Erk1/2 activity and the expression of the lymphatic fate marker *prox1a* by regulating *flt4* expression.

RESULTS

par1 is required for trunk lymphatic development in zebrafish embryos

PCV acts as a source of trunk lymphatic progenitors in zebrafish embryos (Yaniv et al., 2006). Interestingly, our results from whole-mount *in situ* hybridization (WISH) showed that *par1* is highly expressed in the PCV region of zebrafish embryos at 26 hpf (Figure 1A), consistent with a previous report (Xu et al., 2011). Hence, *par1* could be involved in lymphatic development during embryogenesis in zebrafish. To investigate this, we successfully generated a zebrafish mutant of *par1* harboring a 103 bp deletion within its exon 2 using CRISPR/Cas9 technology (Figure 1B). We found that F_2-generation embryos of the mutants seemed to be normal without any severe defects (Figure 1C). However, at 5 dpf, they showed impaired TD formation (Figures 1D and 1F). In siblings, only 6% of somites lacked TDs (Figures 1D and 1F). In contrast, nearly 25% of somites in *par1* zebrafish mutants lacked them (Figures 1D and 1F). In addition, mutants had an average of only 11.2 number of LEC nuclei/6 somites (Figures 1E and 1G), significantly less than 17.5 found in sibling embryos (Figures 1E and 1G).

Taken together, these results confirmed that *par1* is required for TD formation, which implies that it is involved in the development of the lymphatic trunk during zebrafish embryogenesis.

par1 regulates the differentiation of lymphatic progenitors in zebrafish

During the lymphatic development of zebrafish, Prox1a-positive endothelial cells sprout dorsally from the PCV at 30 hpf and form PLs as a pool of lymphatic progenitors at 48 hpf. At the same time, VECs sprout to form the venous intersegmental vessel (vISV) in parallel, which then fuses with the arterial intersegmental vessel (aISV) to establish a circulatory network with alternating arterial and venous connections (Mulligan and Weinstein, 2014; Semo et al., 2016). To determine whether *par1* is involved in lymphatic differentiation,

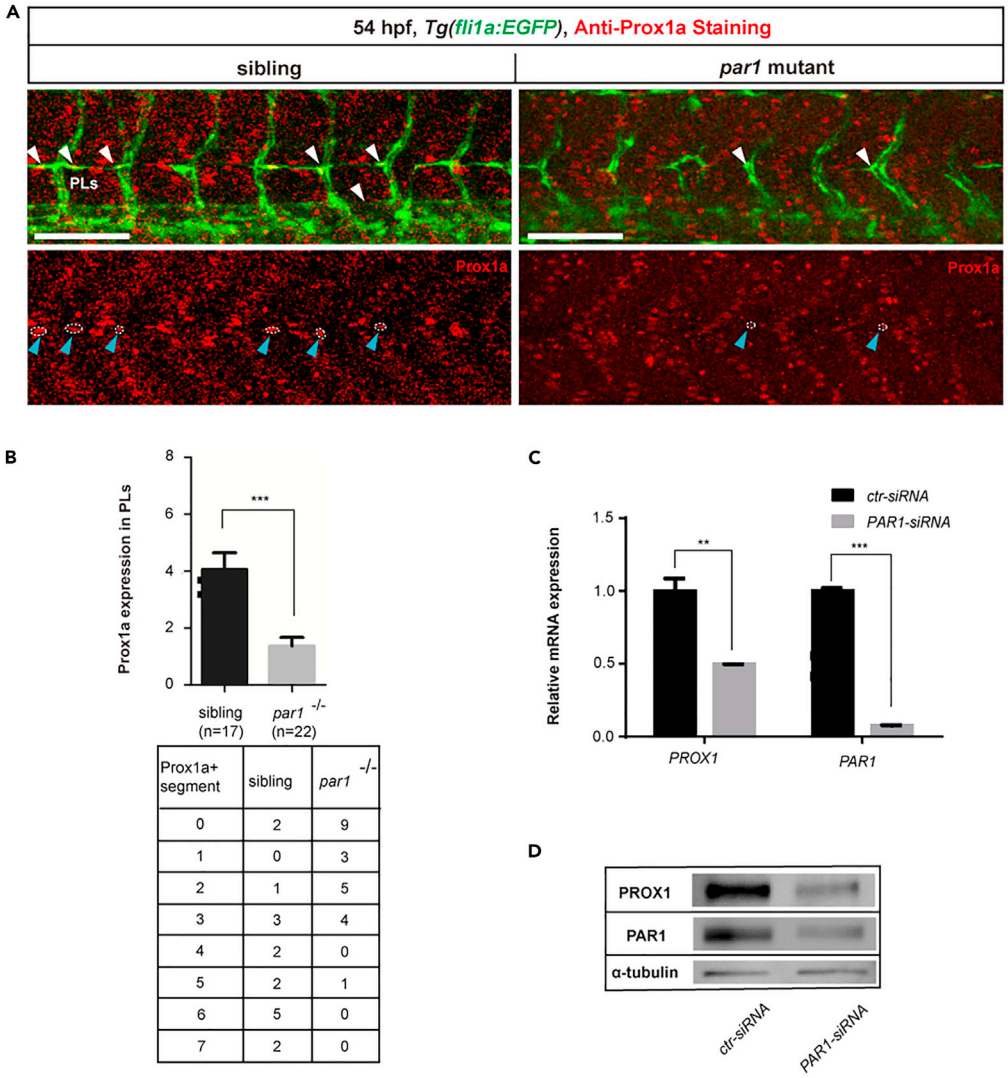

Prox1a+ segment	sibling	par1 -/-
0	2	9
1	0	3
2	1	5
3	3	4
4	2	0
5	2	1
6	5	0
7	2	0

Figure 2. *par1* is required for lymphatic differentiation in zebrafish embryos

(A) Immunostaining of prospero homeobox protein-1a (Prox1a) in *Tg(fli1a:EGFP)* siblings and par1 homozygous mutants at 54 hpf. White arrowheads indicate the presence of parachordal lymphangioblasts (PLs) sprouting in each somite; blue arrowheads with white dashed lines represent positive Prox1a staining in PLs. Scale bars: 100 μm.

(B) Prox1a-positive PLs in siblings (n = 17 embyos) and *par1* homozygous mutants (n = 22 embryos) at 54 hpf; 7 somites/embryos were used for quantification. Table shows the number of prox1a-positive segment per 7 somites in each embryo.

(C) Relative mRNA expression of *PROX1* and *PAR1* in human dermal lymphatic endothelial cells (HDLECs) after *ctr-siRNA* (control) and *PAR1-siRNA* transfection.

(D) Western blot analysis of PROX1 and PAR1 expression upon *PAR1* knockdown in HDLECs. In (C and D), values represent means ± SEMs. *p ≤ 0.01, **p ≤ 0.001 in the Student's t test.

we first performed a whole embryo immunostaining assay to examine expression of Prox1a in PLs of *Tg(fli1a:EGFP)* line at 54 hpf. Compared with sibling embryos, *par1* zebrafish mutants showed a comparable reduction of *prox1a* expression in PLs (Figures 2A and 2B). Concomitant with the role of *par1* in regulating *prox1*a expression in zebrafish embryos, we knocked down the expression of *PAR1* in human dermal lymphatic endothelial cells (HDLECs) using an siRNA method. Interestingly, the expression of *PROX1* significantly decreased not only in terms of mRNA levels (Figure 2C) but also in terms of protein levels (Figure 2D). These results suggest a conserved role of *PAR1* in regulating *PROX1* expression *in vivo* and *in vitro*. To determine whether *par1* is involved in venous and lymphatic sprouting in an earlier stage, we crossed par1 mutant with the *Tg(lyve1b:dsRed;flk1:EGFP)* line, in which *lyve1b:dsRed* labels both venous and

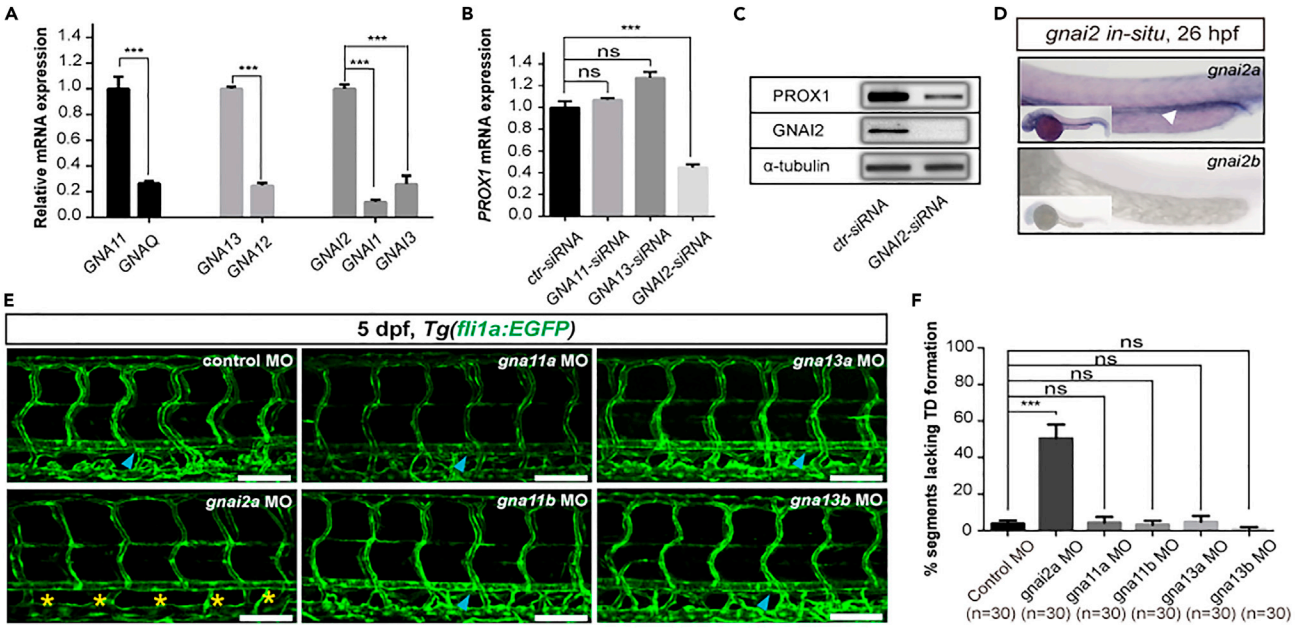

Figure 3. *gnai2a* is selectively required for lymphatic development in zebrafish embryos

(A) Relative mRNA expression of different G-protein-coupled receptors in HDLECs.

(B) Relative mRNA expression of *PROX1* in HDLECs upon transfection with ctr-siRNA (control), GNA11-siRNA, GNA13-siRNA, and GNAI2-siRNA.

(C) Western blot analysis of PROX1 and GNAI2 expression upon *GNAI2* knockdown in HDLECs.

(D) WISH of *gnai2a* gene expression (upper) and *gnai2b* gene expression (below) at 26 hpf in zebrafish embryos. The white arrowhead indicates the PCV area.

(E) Confocal images showing TD formation in *Tg(fli1a:EGFP)* injected with 4 ng control MO, 4 ng *gnai2a* MO, 4 ng *gnai11a* MO, 4 ng *gnai11b* MO, 4 ng *gna13a* MO, and 4 ng *gna13b* MO at 5 dpf. Scale bars: 100 μm.

(F) Percentage of somites lacking TD formation. For each group, 30 embryos were quantified, and 6 somites/embryo were used for quantification. In (A), (B), and (F), values represent means ± SEMs. *p ≤ 0.001; ns, not significant in Student's t test.

lymphatic vessels. Sibling showed almost 100% venous and lymphatic sprouting from the PCV at 36 hpf (Figures S1A and S1B), whereas the *par1* mutants showed only about 80% at the same stage (Figures S1A and S1B). Together, these results demonstrate that *par1* is required for the differentiation of lymphatic progenitors in zebrafish embryos.

gnai2a is selectively required for trunk lymphatic development in zebrafish embryos

A number of different guanine-nucleotide-binding G-protein α-subunits function as downstream effectors of *PAR1*, including members of the G_I, $G_{q/11}$, and $G_{12/13}$ sub-families (Soh et al., 2010; Zhao et al., 2014). In seeking an alternative G protein involved in *par1*-mediated lymphangiogenesis in zebrafish embryos, we first performed quantitative real-time PCR (qPCR) analysis of HDLECs using seven G proteins from different subclasses including *GNAQ*, *GNA11*, *GNA12*, *GNA13*, *GNAI1*, *GNAI2*, and *GNAI3*. We found that only *GNA11*, *GNA13*, and *GNAI2* had a relatively high mRNA expression level (Figure 3A). Then, we knocked down the expression of these three genes in HDLECs using an siRNA method and validated the expression level of *PROX1*. Surprisingly, the results showed that only knockdown of *GNAI2* caused a significant decrease in *PROX1* expression in terms of both mRNA (Figure 3B) and protein levels (Figure 3C). This indicates that *GNAI2* is more likely to be involved in regulating lymphatic differentiation than other G proteins.

Next, we analyzed the expression pattern of *gnai2* homologous genes (*gnai2a* and *gnai2b*) in zebrafish embryos via WISH. The results showed that *gnai2a*, but not *gnai2b*, is highly expressed in the PCV region in which the lymphatic trunk originated at 26 hpf (Figure 3D). To support this result, we then carried out knockdown assays by injecting *gna11a* MO, *gna11b* MO, *gna13a* MO, *gna13b* MO, as well as *gnai2a* MO into embryos in the one-cell stage. We inspected TD formation at 5 dpf in each respective zebrafish morphant. Interestingly, we discovered that only *gnai2a* morphants exhibited defective TD formation, with more than 50% of somites lacking TDs (Figures 3E and 3F). In contrast, control embryos and *gna11a*, *gna11b*, *gna13a*,

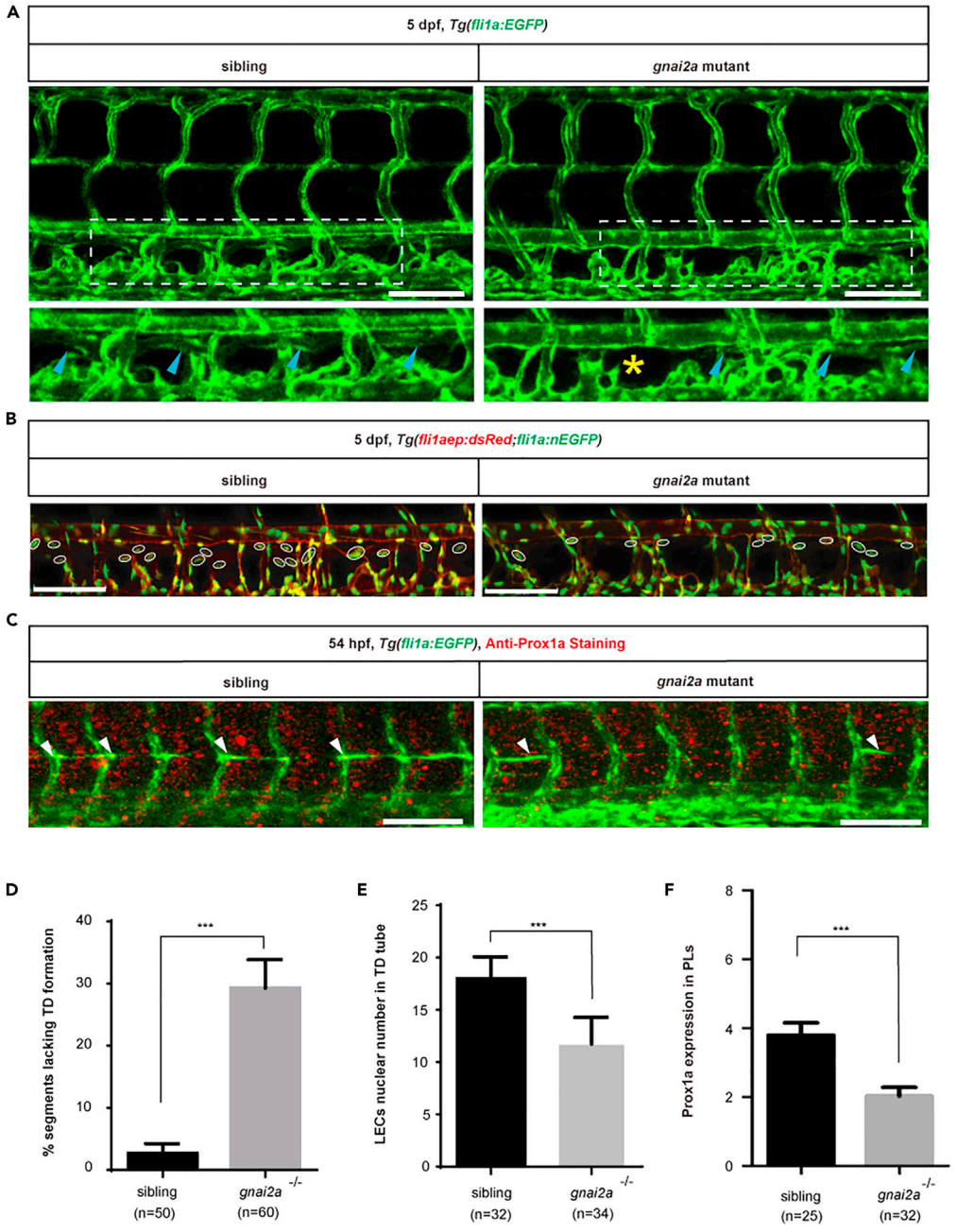

Figure 4. *gnai2a* mutant mimics the lymphatic phenotypes observed in the *par1* mutant

(A) Confocal images showing TD formation in *Tg(fli1a:EGFP)* siblings and gnai2a homozygous mutants at 5 dpf. Blue arrowheads indicate TD formation in each somite; yellow asterisks represent the absence of TD formation in each somite. Scale bars: 100 μm.

(B) Confocal images showing LECs nuclear numbers in the TD tube of siblings and *gnai2a* homozygous mutants in the *Tg(fli1aep:dsRed;fli1:nEGFP)* line at 5 dpf. White circles indicate the presence of LECs nuclear numbers in the TD tube. Scale bars: 100 μm.

(C) Immunostaining of Prox1a of siblings and *gnai2a* homozygous mutants in the *Tg(fli1a:EGFP)* line at 54 hpf. White arrowheads indicate positive Prox1a staining in PLs. Scale bars: 100 μm.

(D) Percentage of somites lacking TD formation in siblings (n = 50) and *gnai2a* homozygous mutants (n = 60 embryos); 6 somites/embryos were used for quantification.

(E) LEC nuclear number in the TD tube of siblings (n = 32) and *gnai2a* homozygous mutants (n = 34 embryos); 6 somites/embryos were used for quantification.

Figure 4. *Continued*
(F) Prox1a-positive PLs of siblings (n = 25) and *gnai2a* homozygous mutants (n = 32 embryos) at 54 hpf; 7 somites/embryos were used for quantification. In (D–F), values represent means ± SEMs. *p ≤ 0.001 in the Student's t test. See also Figures S2–S4.

and *gna13b* morphants showed normal TD formation (Figures 3E and 3F). These results indicate that *gnai2a* is selectively required for lymphatic development in zebrafish embryos.

gnai2a recapitulates *par1*-mediated phenotypes during lymphatic development in zebrafish

To investigate the role of *gnai2a* during zebrafish lymphangiogenesis, we used CRISPR/Cas9 technology to obtain a *gnai2a* mutant harboring a 68 bp deletion in its exon 3 (Figure S2A). The F_2 generations of most mutants had normal phenotypes at 5 dpf (Figure S2B). Next, we examined TD formation at 5 dpf during embryogenesis. As shown in Figure 4, nearly 30% of somites lacked TDs in the mutants, significantly more than sibling embryos. In addition, we assessed the number of LEC nuclei/6 somites in TD tubes at 5 dpf using the transgenic zebrafish line *Tg(fliaep:dsRed;fli1a:nEGFP)*. The mutants had notably decreased numbers, with an average of 11.7 compared with an average of 18.2 in sibling embryos (Figures 4B and 4E).

To evaluate whether *gnai2a* is required to regulate lymphatic differentiation, we conducted an immunostaining assay using anti-Prox1 antibody at 54 hpf in *Tg(fli1a:EGFP)* embryos. We found that F_2 generations of mutants had fewer *prox1a*-positive PLs than sibling embryos (Figures 4C and 4F). Meanwhile, we found that knockdown of *gnai2a* caused a partial failure in the formation of lympho-venous sprouting at 36 hpf, compared with control embryos with normal sprouting (Figures S3A and S3B). This suggests that *gnai2a* is required for lymphatic differentiation in zebrafish.

To further validate that *gnai2a* is the downstream effector of *par1* in this process, we cross-bred *par1* heterozygous mutant and *gnai2a* heterozygous mutant using the *Tg(fli1a:EGFP)* line and *Tg(fli1aep:dsRed;fli1:nEGFP)* line. We found that wild-type embryos, *par1* heterozygous mutants, *gnai2a* heterozygous mutants, and cross-bred *par1-gnai2a* heterozygous mutants had normal morphologies (Figure S4E) and did not display a comparable difference in TD formation (Figures S4A and S4C). However, interestingly, we found that the average number of LEC nuclei/6 somites in the cross-bred mutants was 13.2, compared with 17.6 in wild-type embryos and about 15 in each *par1* heterozygous mutant and *gnai2a* heterozygous mutant (Figures S4B and S4D). This indicates that there is a genetic interaction between *par1* and *gnai2a* in cross-bred *par1-gnai2a* heterozygous zebrafish mutants, especially at the cellular level.

Taken together, these results show that the *gnai2a* zebrafish mutant mimics the phenotypes of *par1* zebrafish mutants, indicating that *gnai2a* is the downstream effector of *par1* in the regulation of zebrafish lymphangiogenesis.

Thrombin is not involved in zebrafish lymphangiogenesis

F2 was the first ligand to be reported to have the ability to cleave and activate PAR1 at a canonical site (Vu et al., 1991). To elucidate whether F2 is required for lymphatic development in zebrafish embryos, we injected F2 MO into embryos (4 ng/embryo) in the one-cell stage. At 5 dpf, we analyzed TD formation and unexpectedly found that both control and F2 morphants had normal TD formation (Figures S5A and S5C). To further validate this result, we treated zebrafish embryos with SCH79797, a specific PAR1 antagonist that blocks the interaction between F2 and PAR1. Consistent with the above results, both treated and vehicle control embryos exhibited normal TD formation at 5 dpf (Figures S5B and S5D), suggesting that *par1* is independent of F2 in regulating lymphatic development in zebrafish. These results clearly indicate that F2 is not required for lymphatic development in zebrafish.

Noncanonical *mmp13b* is required for lymphatic development in zebrafish

Several proteases cleave and activate PAR1, including F2, plasmin, activated protein C, thrombocytin, factor Xa, factor VIIa, tryptase, trypsin, MMPs, and so on (Zhao et al., 2014). To search for candidate proteases involved in PAR1 regulation of lymphangiogenesis in zebrafish, we first conducted qPCR analyses of HDLECs and observed the relative mRNA expression of these proteases. Interestingly, MMP1 showed the highest relative mRNA expression (Figure 5A). Next, we transfected *MMP1*-siRNA into HDLECs and evaluated the expression of *PROX1*. Interestingly, knockdown of *MMP1* caused a significant reduction of *PROX1* mRNA expression, suggesting that MMP1 may be involved in lymphangiogenesis (Figure 5B).

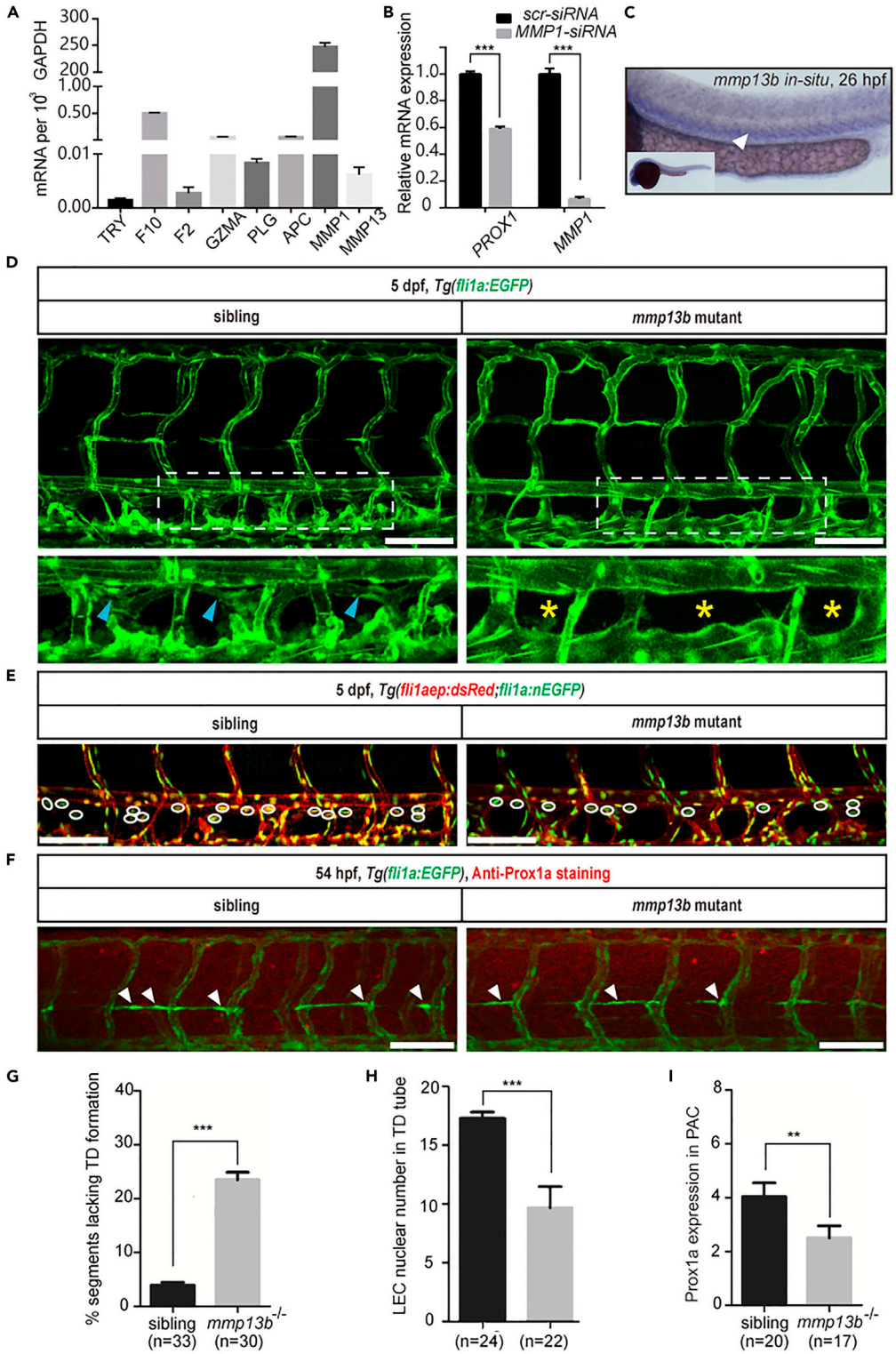

Figure 5. *mmp13b* mutant mimics the lymphatic phenotypes observed in the *par1* mutant

(A) Relative mRNA expression of different PAR1 proteases in HDLECs.

(B) Relative mRNA expression of *PROX1* and *MMP1* in HDLECs after *ctr-siRNA* (control) and *MMP1-siRNA* transfection.

(C) WISH of *mmp13b* gene expression in zebrafish at 26 hpf. The white arrowhead indicates the expression of the *mmp13b* gene in the PCV area.

Figure 5. *Continued*

(D) Confocal images showing TD formation in *Tg(fli1a:EGFP)* siblings and *mmp13b* homozygous mutants at 5 dpf. Blue arrowheads indicate TD formation in each somite; yellow asterisks represent the absence of TD formation in each somite; DA and PCV areas are denoted. Scale bars: 100 μm.

(E) Confocal images showing LECs nuclear numbers in the TD tube of siblings and *mmp13b* homozygous mutants in the *Tg(fli1aep: dsRed;fli1:nEGFP)* line at 5 dpf. White circles indicate the presence of LECs nuclear numbers in the TD tube. Scale bars: 100 μm.

(F) Immunostaining of Prox1a of siblings and *mmp13b* homozygous mutants in the *Tg(fli1a:EGFP)* line at 54 hpf. White arrowheads indicate Prox1a-positive staining in the PLs. Scale bars: 100 μm.

(G) Percentage of somites lacking TD formation in siblings (n = 33 embryos) and *mmp13b* homozygous mutants (n = 30 embryos); 6 somites/embryos were used for quantification.

(H) LEC nuclear numbers in the TD tube of siblings (n = 24 embryos) and *mmp13b* homozygous mutants (n = 22 embryos); 6 somites/embryos were used for quantification.

(I) Prox1a-positive PLs in siblings (n = 20 embryos) and *mmp13b* homozygous mutants (n = 17 embryos) at 54 hpf; 7 somites/embryos were used for quantification. In (G–I), values represent means ± SEMs. *p ≤ 0.01, **p ≤ 0.001 in Student's t test. See also Figures S5 and S6.

In the human genome, there are three collagenases (MMP1, MMP8, and MMP13). However, two of them (Mmp1 and Mmp8) have no zebrafish homolog, and only MMP13 is present in duplicate (Mmp13a and Mmp13b) in the zebrafish genome (Wyatt et al., 2009). *mmp13a* is expressed in myeloid lineage cells but not in the vein (Qian et al., 2005). Therefore, we speculated that *mmp13b* could replace the function of the human *MMP1* gene to regulate *par1*-mediated lymphatic development in zebrafish embryos. We used WISH to observe the expression patterns of *mmp13b* during zebrafish embryogenesis. Interestingly, we found that it is highly expressed in the PCV region at 26 hpf, suggesting that it is involved in lymphatics (Figure 5C). Next, we generated a zebrafish *mmp13b* mutant using CRISPR/Cas9 technology and obtained a stable mutant harboring a 7 bp deletion in its exon 4 (Figure S6). To validate the role of *mmp13b* in regulating lymphangiogenesis, we examined TD formation in the F_2 generation of embryos. As observed in the *par1* zebrafish mutant, *mmp13b* mutant embryos showed nearly 25% of somites lacking TD at 5 dpf, compared with siblings with normal TD formation (Figures 5D and 5G). We also checked the number of LEC nuclei in TD tube with transgenic zebrafish line *Tg(fliaep:dsRed;fli1a:nEGFP)* at 5 dpf and found that the mutant had significantly fewer numbers than sibling embryos (Figures 5E and 5H). Furthermore, immunostaining assays of Prox1a expression in PLs at 54 hpf indicated that mutants also showed significantly reduced Prox1a expression compared with siblings (Figures 5F and 5I). Together, those data demonstrate that *mmp13b* is required for lymphatic development in zebrafish.

Overexpression of cleaved *par1* recovers the phenotypes of *mmp13b* mutant in zebrafish lymphangiogenesis

As observed with the tethered ligand sequence (SFLLRN) in human PAR1, zebrafish Par1 also harbors a putative tethered ligand sequence (SFSGFFL) within the extracellular N-terminal region (Kim et al., 2009; Xu et al., 2011), which can induce thrombocyte activation (Kim et al., 2009). Meanwhile, MMP-13 can cleave PAR1 at the $S_{42}\downarrow_{43}$FLLRN site, and cleaved PAR1 changes its conformation and activates downstream ERK1/2 signaling in cardiac cells (Jaffré et al., 2012). To confirm the function of *mmp13b* as an upstream *par1* protease that regulates lymphatic development in zebrafish, we generated a zebrafish transgenic line, *Tg(lyve1b:cleaved-par1-P2A-mCherry)*, in which cleaved Par1 at the S↓FSGFFL site (named *cleaved-par1*) was fused into *cleaved-par1-P2A-mCherry* and was driven by the venous and lymphatic promoter *lyve1b*. Then we crossed *mmp13b* mutant with the *Tg(lyve1b:cleaved-par1-P2A-mCherry)* or *Tg(lyve1b:mCherry)* line for rescue experiments. We examined TD formation at 5 dpf both for the *mmp13b* zebrafish mutant and siblings in these two transgenic lines. Compared with the normal TD formation of siblings in the *Tg(lyve1b:mCherry)* line at 5 dpf, the *mmp13b* zebrafish mutant lacked TD at 5 dpf (Figures 6A and 6B). Meanwhile, overexpression of *par1* under the *lyve1b* promoter did not induce ectopic TD formation, and overexpression showed a normal TD morphology (Figures 6A and 6B). However, the mutant in the *Tg(lyve1b:cleaved-par1-P2A-mCherry)* background showed normal TD formation (Figures 6A and 6B), indicating that the overexpression of *par1* in the *mmp13b* zebrafish mutant can recover the defect phenotype. Hence, *mmp13b* could serve as an upstream *par1* protease that regulates lymphatic development in zebrafish embryos.

par1 promotes Erk1/2 activity and *flt4* expression in zebrafish embryos

Vegfc and its receptor Flt4 activate p-Erk1/2 by inducing *prox1a* expression, ultimately regulating the differentiation of lymphatic progenitor cells in zebrafish embryos (Koltowska et al., 2015; Küchler et al., 2006;

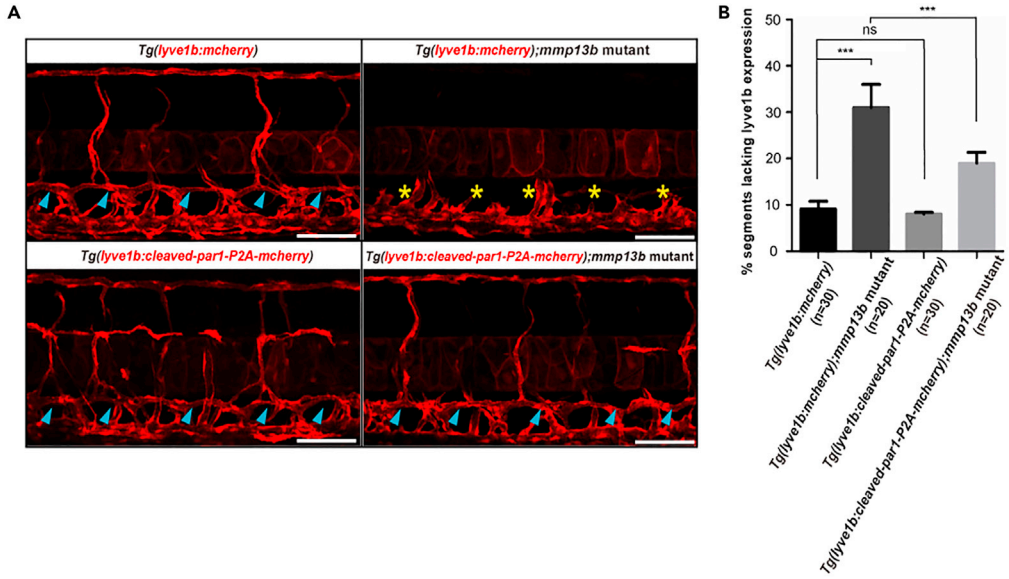

Figure 6. Overexpression of cleaved *par1* recovers the lymphatic phenotypes observed in *mmp13b* zebrafish mutants

(A) Confocal images showing TD formation of siblings and *mmp13b* homozygous mutants in the *Tg(lyve1b:mcherry)* line and *Tg(lyve1b:cleaved-par1-P2A-mcherry)* line at 5 dpf. Blue arrowheads indicate TD formation in each somite; yellow asterisks represent the absence of TD formation in each somite. Scale bars: 100 μm.

(B) Percentage of somites lacking TD formation in siblings with the *Tg(lyve1b:mcherry)* line (n = 30 embryos), mmp13b homozygous mutants with the *Tg(lyve1b:mcherry)* line (n = 20 embryos), siblings with the *Tg(lyve1b:cleaved-par1-P2A-mcherry)* line (n = 30 embryos), and mmp13b homozygous mutants with the *Tg(lyve1b:cleaved-par1-P2A-mcherry)* line (n = 20 embryos); 6 somites/embryos were used for quantification. In (B), values represent means ± SEMs. *$p \leq 0.01$, **$p \leq 0.001$ in the Student's t test.

Shin et al., 2016). Based on our above results, we propose that *par1* may promote Vegfc/Flt4/Erk signaling activity to regulate lymphangiogenesis in zebrafish embryos. To test this hypothesis, we performed a whole-embryo p-Erk1/2 immunostaining assay using the F_2 generations of *Tg(fli1a:EGFP)* embryos. At 28 hpf, when lymphatic progenitors start migrating dorsally from the PCV, we observed clear p-Erk1/2 staining in the PCV of sibling embryos (Figures 7A and 7B). However, there was significantly less staining in the PCV of *par1* zebrafish mutants (Figures 7A and 7B). Next, to confirm whether *PAR1* promotes VEGFC-induced p-ERK1/2 activation, we performed *PAR1* knockdown experiments in cultured HDLECs and found that knockdown of PAR1 caused a significant decrease in *VEGFR3* mRNA level (Figure 7C). We then evaluated the effect of PAR1 on VEGFC-induced phosphor-ERK1/2 activity in HDLECs *in vitro*. In HDLECs transfected with control-siRNA (ctr-siRNA), a significant increase in ERK1/2 phosphorylation was detected at 15 min. In contrast, HDLECs transfected with *PAR1*-siRNA showed a significant decrease in p-ERK1/2 levels (Figure 7D). Meanwhile, knockdown of PAR1 also caused a compromised VEGFR3 expression at the protein level (Figure 7D).

In parallel, we also examined the expression of *flt4* during zebrafish embryogenesis. The results from qPCR analysis showed that loss of *par1* function decreased *flt4* mRNA levels in zebrafish embryos (Figure 7E). Meanwhile, *par1* mutants clearly showed a reduction in *flt4* expression at 28 hpf, compared with sibling in the same stage (Figure 7F). Transcription factor *hhex* has been reported to regulate *flt4* mRNA levels in the PCV during the lymphatic development of zebrafish (Gauvrit et al., 2018). To determine whether *par1* regulates *hhex* expression in zebrafish embryos, we performed WISH tests. *par1* mutants showed decreased *hhex* expression in the PCV at 28 hpf, compared with siblings (Figure 7F). Together, these results demonstrate that *par1* promotes *flt4* expression during lymphatic development in zebrafish.

DISCUSSION

The PAR family, especially PAR1, is a critical mediator of vascular hemostasis, thrombosis, and inflammation (Alberelli and De Candia, 2014). Here, we found compelling evidence that the noncanonical

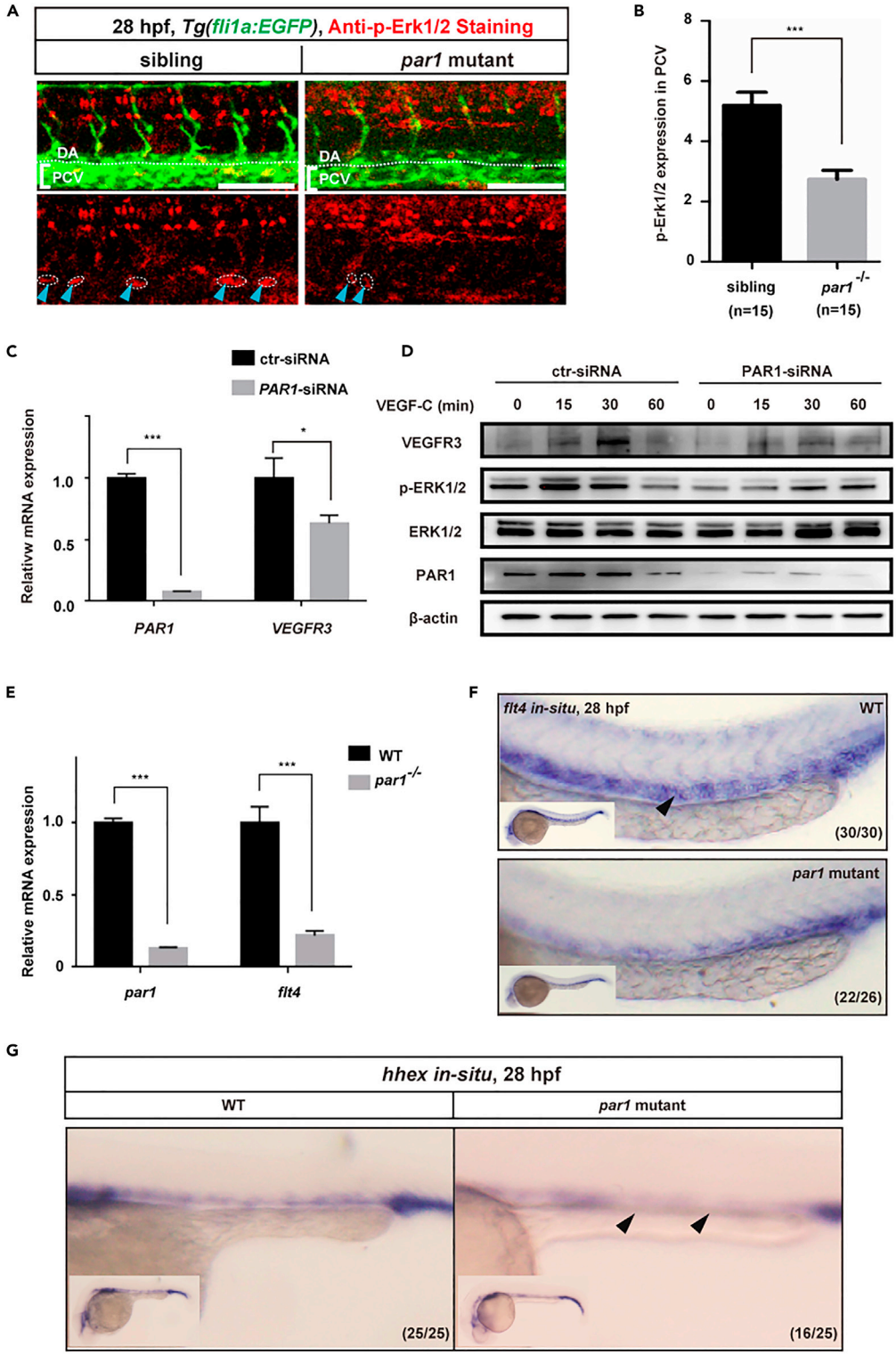

Figure 7. Loss of *par1* function decreases p-Erk1/2 activity and *flt4* expression in the PCV of zebrafish embryos

(A) Immunostaining of phosphoErk1/2 (p-Erk1/2) activity in *Tg(fli1a:EGFP)* siblings and par1 homozygous mutants at 28 hpf. Blue arrowheads with white dashed lines indicate positive p-Erk1/2 staining; DA and PCV (in brackets) area are noted. Scale bars: 100 μm.

Figure 7. *Continued*

(B) Quantification of p-Erk1/2 expression staining in the PCV of siblings (n = 15 embryos) and *par1* mutants (n = 15 embryos); 8 somites/embryos were used for quantification.

(C) Relative mRNA expression of *VEGFR3* in HDLECs after *ctr-siRNA* (control) and *PAR1-siRNA* transfection.

(D) Western blot analysis of p-ERK1/2 activity in HDLECs transfected with ctr-siRNA or PAR1-siRNA, followed by VEGFC treatment.

(E) Relative mRNA expression of the *flt4* gene in siblings and *par1* homozygous zebrafish embryo mutants.

(F) WISH of *flt4* gene expression at 28 hpf in wild-type and *par1* homozygous mutant embryos. The white arrowhead indicates the PCV area.

(G) WISH of *hhex* gene expression at 28 hpf in wild-type and *par1* mutant embryos. The white arrowhead indicates the PCV area. In (B, C, and, E), values represent means ± SEMs. *p ≤ 0.05, **p ≤ 0.001, ***p ≤ 0.0001 in the Student's t test.

Mmp13b-Par1-Gnai2a axis regulates the differentiation of trunk lymphatic progenitors by promoting *flt4* expression in the PCV in the early stage (Figure 8).

In zebrafish embryos, trunk lymphatic progenitors originate from the PCV (Yaniv et al., 2006), suggesting that genes enriched in the PCV may be involved in lymphangiogenesis in zebrafish. We found several lines of evidence that *par1* regulates lymphatic differentiation in zebrafish. First, *par1* is highly enriched in the PCV at 26 hpf. Second, *par1* regulates prox1 expression *in vitro* and *in vivo*. Third, *par1* mutant shows decreased *flt4* expression and compromised phospho-Erk1/2 activity in the PCV, both of which are crucial for lymphatic differentiation in zebrafish embryos (Koltowska et al., 2015; Shin et al., 2016). However, both defective venous-lymphatic sprouting and subsequent compromised TD formation are mild in the *par1* mutant, whereas *par1* homozygous mutants showed clear reduction in *prox1a* expression in PLs at 54 hpf and in the nucleus number of LECs in TD tubes at 5 dpf. These results suggest that *par1* plays an important role in lymphatic differentiation rather than in lymphatic migration in zebrafish embryos. Consistent with this, *prox1a* mutant zebrafish embryos show normal TD formation (van Impel et al., 2014), whereas maternal and zygotic *prox1a* mutant zebrafish show a significant decrease in number of LEC nuclei (Koltowska et al., 2015).

Several G proteins (including GNA12/13, GNAQ/11, and GANI1/2/3) function as downstream effectors of PAR1 (Zhao et al., 2014). Here, we demonstrated that *gnai2a* is selectively required for *par1*-mediated lymphatic development in zebrafish embryos. Furthermore, *gnai2a* mutants mimicked the phenotypes observed in *par1* mutants in terms of lymphatic development. We also performed genetic interaction analyses by cross-breeding *par1* heterozygous zebrafish mutant and *gnai2a* heterozygous zebrafish mutants. The morphologies of the embryos did not show any significant differences at 5 dpf, compared with wild-type embryos. However, nucleus counting at 5 dpf indicated significantly fewer number of LEC nuclei in the *par1-gnai2a* heterozygous mutant embryos. This indicates that there is a genetic interaction at the cellular level between *par1* and *gnai2a*.

Several PAR1 upstream proteases have been identified, such as F2, plasmin, factor Xa, factor VIIa, trypsin, MMPs, and others (Zhao et al., 2014). Surprisingly, canonical F2 was not involved in lymphatic development in zebrafish embryos. Although human MMP1 regulates PROX1 expression in HDLECs *in vitro*, our results strongly suggest that *mmp13* serves as an upstream protease of *par1* that regulates lymphatic development in zebrafish. In mice, there is no *mmp1* gene, and MMP13 is thought to play the role of human MMP1, cleaving and activating PAR1 at the conserved $S_{42}\downarrow_{43}$FLLRN site (Jaffré et al., 2012). In zebrafish, two orthologs of MMP13 (Mmp13a, Mmp13b) are present (Wyatt et al., 2009). *mmp13a* is expressed in myeloid lineage cells but not in the vein (Qian et al., 2005). Interestingly, we found that *mmp13b* is highly expressed in the PCV region of zebrafish embryos at 26 hpf. Furthermore, we found that zebrafish *mmp13b* mutants perfectly mimicked the phenotypes of *par1* zebrafish mutants. Further analysis also revealed that the overexpression of cleaved *par1* in *mmp13b* zebrafish mutants rescued the defective TD phenotype. These results suggest the *mmp13b* acts upstream of *par1* to regulate lymphatic development in zebrafish embryos.

During LEC progenitors differentiation, these Prox1-positive cells migrate dorsally out of PCV, sprouting in response to signaling induced by VEGFC, through its receptor VEGFR3 or FLT4 to form the first lymphatic vessels (Haiko et al., 2008; Hogan et al., 2009a, 2009b; Karkkainen et al., 2004; Küchler et al., 2006). Disruption of *vegfc* or *flt4* causes a severe defect in the lymphatic development of zebrafish and mice (Hogan et al., 2009a, 2009b; Karkkainen et al., 2004; Küchler et al., 2006; Villefranc et al., 2013; Yaniv et al., 2006). Further, Vegfc/Flt4 signaling can induce *prox1a* expression through Erk1/2, therefore initiating the differentiation and sprouting of lymphatic endothelial cells in the lymphatic trunk of zebrafish (Shin et al., 2016).

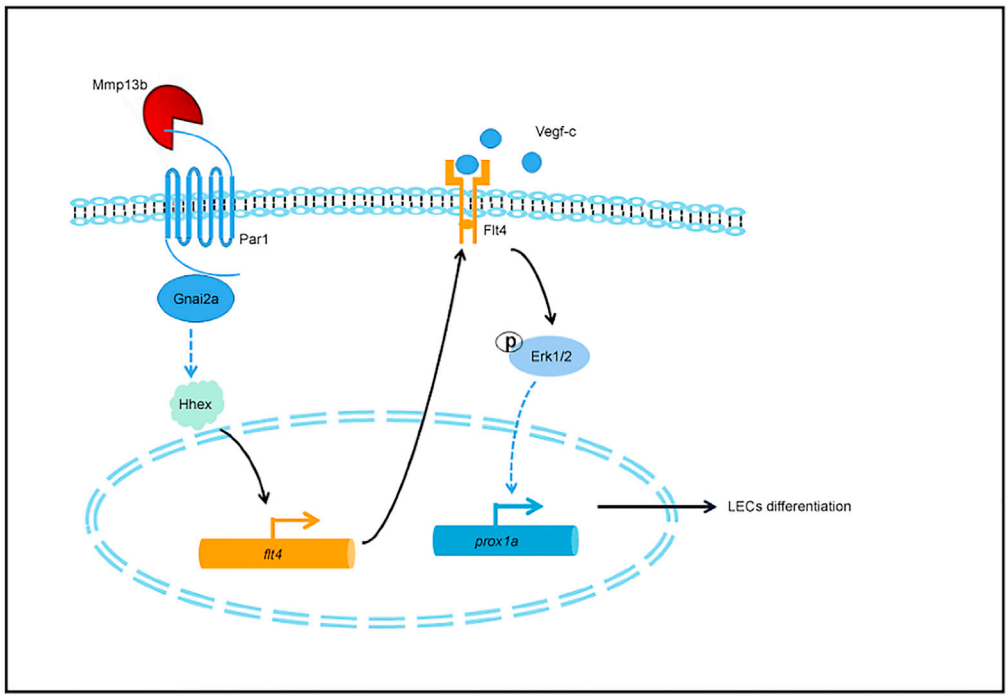

Figure 8. Work model

The mmp13b-Par1-Gnai2a axis regulates *flt4* expression in the PCV in early stage zebrafish embryos probably through hhex transcription factor, therefore indirectly regulating *prox1a* expression and promoting the differentiation of lymphatic trunk progenitors.

In our study, we found several lines of evidence indicating that *par1* regulates Vegfc/*Flt4/Erk1/2* signaling during lymphatic development in zebrafish. First, loss of the *par1* gene reduced *flt4* expression. Second, the *par1* zebrafish mutant showed decreased expression of hhex, an upstream transcription factor of *flt4* in zebrafish embryos (Gauvrit et al., 2018). Third, disruption of *par1* inhibited phospho-Erk1/2 activities in the PCV of zebrafish embryos and VEGFC-induced phospho-ERK1/2 activity *in vitro*. A high level of VEGFR3/FLT4 may be a crucial prerequisite for the sensitivity of LEC progenitors to the VEGF-C induction (Ducoli and Detmar, 2021). Consistent with this, our zebrafish *par1* mutant showed significantly less prox1 expression and compromised *flt4* expression. In contrast, disruption of the *par1* gene caused a mild defect in venous-lymphatic sprouting and in subsequent TD formation. We speculate that high expression of *flt4* is much more sensitive to lymphatic differentiation than that to venous-lymphatic sprouting in zebrafish embryos. Previous document reported that *flt4* null mutant showed clear edema, whereas $flt4^{Y1226/7\Delta}$ mutants have no edema (Shin et al., 2016). Further analysis revealed signaling through *flt4* Y1226/7 and ERK is required for trunk lymphatic development but not for facial lymphatic formation. This indicated that facial lymphatic vessels, but not the thoracic duct, are initially dispensable for lymphatic function in zebrafish embryos. In this study, we found that *par1* mutant, *mmp13b* mutant, and *gnai2a* mutant have no edema. It is possibility that *par1* signaling mainly regulated trunk lymphatic development in zebrafish embryos through flt4 and Erk1/2 signaling, which supported the previous notion (Shin et al., 2016).

Taken together, our results uncover a mechanism in which the *mmp13b-par1-gnai2a* axis regulates the lymphangiogenic process in the lymphatic trunk of zebrafish by promoting Vegfc/Flt4/Erk1/2 signaling, which induces *prox1a*. expression.

Limitation of the study

In our study, we generated three mutants and found that *mmmp13b-par1-gnai2a* axis regulates the differentiation of lymphatic progenitors in zebrafish embryos. Mechanistically, *par1* promotes *flt4* expression and phospho-Erk1/2 activity in the posterior cardinal vein. However, the mechanism linking the *mmp13b-par1-gnai2a* pathway to regulation of flt4 would need to be further expanded.

STAR★METHODS

Detailed methods are provided in the online version of this paper and include the following:

- KEY RESOURCES TABLE
- RESOURCE AVAILABILITY
  - Lead contact
  - Materials availability
  - Data and code availability
- EXPERIMENTAL MODEL AND SUBJECT DETAILS
  - Zebrafish
- METHOD DETAILS
  - Generation of the zebrafish transgenic line
  - Generation of zebrafish mutants using CRISPR/Cas9 technology
  - Microinjection of MOs
  - Antagonist exposure
  - Imaging
  - *In situ* hybridization
  - Whole mount immunostaining
  - Cell culture and western blotting
  - Quantitative RT-PCR analysis
- QUANTIFICATION AND STATISTICAL ANALYSIS

SUPPLEMENTAL INFORMATION

Supplemental information can be found online at https://doi.org/10.1016/j.isci.2021.103386.

ACKNOWLEDGMENTS

This study was supported by grants from the National Natural Science Foundation of China (31771599, 31971242), Chongqing Science and Technology Bureau (cstc2019jcyj-zdxmX0028), and the National Key Technology R&D Program of China (2016YFC1102305). The authors want to thank the assistance from the Chongqing Engineering Laboratory in Vascular Implants and the Public Experiment Center of State Bioindustrial Base (Chongqing), China.

AUTHOR CONTRIBUTIONS

Conceptualization, Y.W.; Methodology, D.L., M.A.R., X.Z., Y.M., X.Z., and L.W.; Investigation, Y.W., D.L., M.A.R., and X.Z.; Writing—Original Draft, Y.W., G.W., D.L., and M.A.R.; Writing—Review & Editing, Y.W., G.W., D.L., and M.A.R.; Funding Acquisition, Y.W. and G.W.; Resources, L.L., T.Z., and Y.L. Supervision, Y.W. and G.W. All authors approved the final version of the manuscript.

DECLARATION OF INTERESTS

The authors declare that there is no conflict of interest.

Received: March 30, 2021
Revised: August 26, 2021
Accepted: October 26, 2021
Published: November 19, 2021

REFERENCES

Alberelli, M.A., and De Candia, E. (2014). Functional role of protease activated receptors in vascular biology. Vascul. Pharmacol. *62*, 72–81. https://doi.org/10.1016/j.vph.2014.06.001.

Alitalo, K. (2011). The lymphatic vasculature in disease. Nat. Med. *17*, 1371–1380. https://doi.org/10.1038/nm.2545.

Austin, K.M., Nguyen, N., Javid, G., Covic, L., and Kuliopulos, A. (2013). Noncanonical matrix metalloprotease-1-protease-activated receptor-1 signaling triggers vascular smooth muscle cell dedifferentiation and arterial stenosis. J. Biol. Chem. *288*, 23105–23115. https://doi.org/10.1074/jbc.M113.467019.

Cha, Y.R., Fujita, M., Butler, M., Isogai, S., Kochhan, E., Siekmann, A.F., and Weinstein, B.M. (2012). Chemokine signaling directs trunk lymphatic network formation along the preexisting blood vasculature. Dev. Cell *22*, 824–836. https://doi.org/10.1016/j.devcel.2012.01.011.

Coughlin, S.R. (2005). Protease-activated receptors in hemostasis, thrombosis and vascular biology. J. Thromb. Haemost. *3*, 1800–1814. https://doi.org/10.1111/j.1538-7836.2005.01377.x.

Cui, H., Wang, Y.Y., Huang, H., Yu, W., Bai, M., Zhang, L., Bryan, B.A., Wang, Y.Y., Luo, J., Li, D.,

et al. (2014). GPR126 protein regulates developmental and pathological angiogenesis through modulation of VEGFR2 receptor signaling. J. Biol. Chem. *289*, 34871–34885. https://doi.org/10.1074/jbc.M114.571000.

Ducoli, L., and Detmar, M. (2021). Beyond PROX1: Transcriptional, epigenetic, and noncoding RNA regulation of lymphatic identity and function. Dev. Cell *56*, 406–426. https://doi.org/10.1016/j.devcel.2021.01.018.

Ellertsdottir, E., Berthold, P.R., Bouzaffour, M., Dufourcq, P., Trayer, V., Gauron, C., Vriz, S., Affolter, M., and Rampon, C. (2012). Developmental role of zebrafish protease-activated receptor 1 (PAR1) in the cardio-vascular system. PLoS One *7*, e42131. https://doi.org/10.1371/journal.pone.0042131.

Galt, S.W., Lindemann, S., Allen, L., Medd, D.J., Falk, J.M., McIntyre, T.M., Prescott, S.M., Kraiss, L.W., Zimmerman, G.A., and Weyrich, A.S. (2002). Outside-in signals delivered by matrix metalloproteinase-1 regulate platelet function. Circ. Res. *90*, 1093–1099. https://doi.org/10.1161/01.RES.0000019241.12929.EB.

Gauvrit, S., Villasenor, A., Strilic, B., Kitchen, P., Collins, M.M., Marín-Juez, R., Guenther, S., Maischein, H.M., Fukuda, N., Canham, M.A., et al. (2018). HHEX is a transcriptional regulator of the VEGFC/FLT4/PROX1 signaling axis during vascular development. Nat. Commun. *9*, 2074. https://doi.org/10.1038/s41467-018-05039-1.

Haiko, P., Makinen, T., Keskitalo, S., Taipale, J., Karkkainen, M.J., Baldwin, M.E., Stacker, S.A., Achen, M.G., and Alitalo, K. (2008). Deletion of vascular endothelial growth factor C (VEGF-C) and VEGF-D is not equivalent to VEGF receptor 3 deletion in mouse embryos. Mol. Cell. Biol. *28*, 4843–4850. https://doi.org/10.1128/mcb.02214-07.

Hogan, Benjamin M., Bos, F.L., Bussmann, J., Witte, M., Chi, N.C., Duckers, H.J., and Schulte-Merker, S. (2009a). Ccbe1 is required for embryonic lymphangiogenesis and venous sprouting. Nat. Genet. *41*, 396–398. https://doi.org/10.1038/ng.321.

Hogan, Benjamin M., Herpers, R., Witte, M., Heloterä, H., Alitalo, K., Duckers, H.J., and Schulte-Merker, S. (2009b). Vegfc/Flt4 signalling is suppressed by Dll4 in developing zebrafish intersegmental arteries. Development *136*, 4001–4009. https://doi.org/10.1242/dev.039990.

Hong, Y.K., Harvey, N., Noh, Y.H., Schacht, V., Hirakawa, S., Detmar, M., and Oliver, G. (2002). Prox1 is a master control gene in the program specifying lymphatic endothelial cell fate. Dev. Dyn. *225*, 351–357. https://doi.org/10.1002/dvdy.10163.

Jaffré, F., Friedman, A.E., Hu, Z., MacKman, N., and Blaxall, B.C. (2012). β-Adrenergic receptor stimulation transactivates protease-activated receptor 1 via matrix metalloproteinase 13 in cardiac cells. Circulation *125*, 2993–3003. https://doi.org/10.1161/CIRCULATIONAHA.111.066787.

Jin, S.-W. (2005). Cellular and molecular analyses of vascular tube and lumen formation in zebrafish. Development *132*, 5199–5209. https://doi.org/10.1242/dev.02087.

Karkkainen, M.J., Haiko, P., Sainio, K., Partanen, J., Taipale, J., Petrova, T.V., Jeltsch, M., Jackson, D.G., Talikka, M., Rauvala, H., et al. (2004). Vascular endothelial growth factor C is required for sprouting of the first lymphatic vessels from embryonic veins. Nat. Immunol. *5*, 74–80. https://doi.org/10.1038/ni1013.

Kim, H., Nguyen, V.P., Petrova, T.V., Cruz, M., Alitalo, K., and Dumont, D.J. (2010). Embryonic vascular endothelial cells are malleable to reprogramming via Prox1 to a lymphatic gene signature. BMC Dev. Biol. *10*, 17. https://doi.org/10.1186/1471-213X-10-72.

Kim, S., Carrillo, M., Kulkarni, V., and Jagadeeswaran, P. (2009). Evolution of primary hemostasis in early vertebrates. PLoS One *4*, e8403. https://doi.org/10.1371/journal.pone.0008403.

Koltowska, K., Lagendijk, A.K., Pichol-Thievend, C., Fischer, J.C., Francois, M., Ober, E.A., Yap, A.S., and Hogan, B.M. (2015). Vegfc regulates bipotential precursor division and Prox1 expression to promote lymphatic identity in zebrafish. Cell Rep. *13*, 1828–1841. https://doi.org/10.1016/j.celrep.2015.10.055.

Küchler, A.M., Gjini, E., Peterson-Maduro, J., Cancilla, B., Wolburg, H., and Schulte-Merker, S. (2006). Development of the zebrafish lymphatic system requires vegfc signaling. Curr. Biol. *16*, 1244–1248. https://doi.org/10.1016/j.cub.2006.05.026.

Kwan, K.M., Fujimoto, E., Grabher, C., Mangum, B.D., Hardy, M.E., Campbell, D.S., Parant, J.M., Yost, H.J., Kanki, J.P., and Chien, C.B. (2007). The Tol2kit: A multisite gateway-based construction Kit for Tol2 transposon transgenesis constructs. Dev. Dyn. *236*, 3088–3099. https://doi.org/10.1002/dvdy.21343.

Li, Z., Wang, Y., Zhang, M., Xu, P., Huang, H., Wu, D., and Meng, A. (2012). The Amotl2 gene inhibits Wnt/β-catenin signaling and regulates embryonic development in zebrafish. J. Biol. Chem. *287*, 13005–13015. https://doi.org/10.1074/jbc.M112.347419.

Mulligan, T.S., and Weinstein, B.M. (2014). Emerging from the PAC: Studying zebrafish lymphatic development. Microvasc. Res. *96*, 23–30. https://doi.org/10.1016/j.mvr.2014.06.001.

Nicenboim, J., Malkinson, G., Lupo, T., Asaf, L., Sela, Y., Mayseless, O., Gibbs-Bar, L., Senderovich, N., Hashimshony, T., Shin, M., et al. (2015). Lymphatic vessels arise from specialized angioblasts within a venous niche. Nature *522*, 56–61. https://doi.org/10.1038/nature14425.

Okuda, K.S., Astin, J.W., Misa, J.P., Flores, M.V., Crosier, K.E., and Crosier, P.S. (2012). lyve1 expression reveals novel lymphatic vessels and new mechanisms for lymphatic vessel development in zebrafish. Development *139*, 2381–2391. https://doi.org/10.1242/dev.077701.

Proulx, K., Lu, A., and Sumanas, S. (2010). Cranial vasculature in zebrafish forms by angioblast cluster-derived angiogenesis. Dev. Biol. *348*, 34–46. https://doi.org/10.1016/j.ydbio.2010.08.036.

Qian, F., Zhen, F., Ong, C., Jin, S.W., Soo, H.M., Stainier, D.Y.R., Lin, S., Peng, J., and Wen, Z. (2005). Microarray analysis of zebrafish cloche mutant using amplified cDNA and identification of potential downstream target genes. Dev. Dyn. *233*, 1163–1172. https://doi.org/10.1002/dvdy.20444.

Roman, B.L., Pham, V.N., Lawson, N.D., Kulik, M., Childs, S., Lekven, A.C., Garrity, D.M., Moon, R.T., Fishman, M.C., Lechleider, R.J., et al. (2002). Disruption of acvrl1 increases endothelial cell number in zebrafish cranial vessels. Development *129*, 3009–3019. https://doi.org/10.1242/dev.129.12.3009.

Schulte-Merker, S., Sabine, A., and Petrova, T.V. (2011). Lymphatic vascular morphogenesis in development, physiology, and disease. J. Cell. Biol. *93*, 607–618. https://doi.org/10.1083/jcb.201012094.

Semo, J., Nicenboim, J., and Yaniv, K. (2016). Development of the lymphatic system: New questions and paradigms. Development *143*, 924–935. https://doi.org/10.1242/dev.132431.

Shin, M., Male, I., Beane, T.J., Villefranc, J.A., Kok, F.O., Zhu, L.J., and Lawson, N.D. (2016). Vegfc acts through ERK to induce sprouting and differentiation of trunk lymphatic progenitors. Development *144*, 3785–3795. https://doi.org/10.1242/dev.137901.

Soh, U.J., Dores, M.R., Chen, B., and Trejo, J. (2010). Signal transduction by protease-activated receptors. Br. J. Pharmacol. *160*, 191–203. https://doi.org/10.1111/j.1476-5381.2010.00705.x.

Trivedi, V., Boire, A., Tchernychev, B., Kaneider, N.C., Leger, A.J., O'Callaghan, K., Covic, L., and Kuliopulos, A. (2009). Platelet matrix metalloprotease-1 mediates thrombogenesis by activating PAR1 at a cryptic ligand site. Cell *137*, 332–343. https://doi.org/10.1016/j.cell.2009.02.018.

van Impel, A., Zhao, Z., Hermkens, D.M.A., Roukens, M.G., Fischer, J.C., Peterson-Maduro, J., Duckers, H., Ober, E.A., Ingham, P.W., Schulte-Merker, S., et al. (2014). Divergence of zebrafish and mouse lymphatic cell fate specification pathways. Development *141*, 1228–1238. https://doi.org/10.1242/dev.105031.

Villefranc, J.A., Nicoli, S., Bentley, K., Jeltsch, M., Zarkada, G., Moore, J.C., Gerhardt, H., Alitalo, K., and Lawson, N.D. (2013). A truncation allele in vascular endothelial growth factor c reveals distinct modes of signaling during lymphatic and vascular development. Development *140*, 1497–1506. https://doi.org/10.1242/dev.084152.

Vu, T.K.H., Hung, D.T., Wheaton, V.I., and Coughlin, S.R. (1991). Molecular cloning of a functional thrombin receptor reveals a novel proteolytic mechanism of receptor activation. Cell *64*, 1057–1068. https://doi.org/10.1016/0092-8674(91)90261-V.

Wang, Y., Li, Z., Xu, P., Huang, L., Tong, J., Huang, H., and Meng, A. (2011). Angiomotin-like2 gene (amotl2) is required for migration and proliferation of endothelial cells during angiogenesis. J. Biol. Chem. *286*, 41095–41104. https://doi.org/10.1074/jbc.M111.296806.

Wigle, J.T., Harvey, N., Detmar, M., Lagutina, I., Grosveld, G., Gunn, M.D., Jackson, D.G., and Oliver, G. (2002). An essential role for Prox1 in the induction of the lymphatic endothelial cell phenotype. EMBO J. *21*, 1505–1513. https://doi.org/10.1093/emboj/21.7.1505.

Wigle, J.T., and Oliver, G. (1999). Prox1 function is required for the development of the murine lymphatic system. Cell *98*, 769–778. https://doi.org/10.1016/S0092-8674(00)81511-1.

Wyatt, R.A., Keow, J.Y., Harris, N.D., Haché, C.A., Li, D.H., and Crawford, B.D. (2009). The zebrafish embryo: A powerful model system for investigating matrix remodeling. Zebrafish *6*, 347–354. https://doi.org/10.1089/zeb.2009.0609.

Xu, H., Echemendia, N., Chen, S., and Lin, F. (2011). Identification and expression patterns of members of the protease-activated receptor (par) gene family during zebrafish development. Dev. Dyn. *240*, 278–287. https://doi.org/10.1002/dvdy.22517.

Yaniv, K., Isogai, S., Castranova, D., Dye, L., Hitomi, J., and Weinstein, B.M. (2006). Live imaging of lymphatic development in the zebrafish. Nat. Med. *12*, 711–716. https://doi.org/10.1038/nm1427.

Yue, R., Li, H., Liu, H., Li, Y., Wei, B., Gao, G., Jin, Y., Liu, T., Wei, L., Du, J., et al. (2012). Thrombin receptor regulates hematopoiesis and endothelial-to-hematopoietic transition. Dev. Cell *22*, 1092–1100. https://doi.org/10.1016/j.devcel.2012.01.025.

Zhao, P., Metcalf, M., and Bunnett, N.W. (2014). Biased signaling of protease-activated receptors. Front. Endocrinol. *13*, 67. https://doi.org/10.3389/fendo.2014.00067.

STAR★METHODS

KEY RESOURCES TABLE

REAGENT or RESOURCE	SOURCE	IDENTIFIER
Antibodies		
Recombinant anti-PROX1 antibody	GeneTex	Cat#GTX128354;RRID:AB_2893482
F2R rabbit pAb	ABclonal	Cat#A5641;RRID:AB_2766401
GNAI2 rabbit pAb	ABclonal	Cat#A7676;RRID:AB_2769633
Anti-alpha tubulin antibody	Abcam	Cat#ab18251;RRID:AB_2210057
GAPDH (D16H11) XP® Rabbit mAb	Cell Signaling Technology	Cat#5174;RRID:AB_10622025
p44/42 MAPK (Erk1/2) (137F5) Rabbit mAb	Cell Signaling Technology	Cat#4695;RRID:AB_390779
Phospho-p44/42 MAPK (Erk1/2) (Thr202/ Tyr204) (D13.14.4E) XP® Rabbit mAb	Cell Signaling Technology	Cat#4370;RRID:AB_2315112
ß-actin	ZEN BIO	Cat#380624;RRID:AB_2893488
Goat anti-Mouse IgG (H&L) (HRP conjugate)	ZEN BIO	Cat# 511103;RRID:AB_2893489
Goat anti-rabbit IgG (H+L) secondary antibody 555	ThermoFisher Scientific	Cat#A21434;RRID:AB_2535855
Chemicals, peptides, and recombinant proteins		
TritonX-100	Sigma	T9284
Bovine Serum Albumin	Sigma	A9647
4x protein loading buffer	Li-cor	928-40004
PTU	Sigma	2954-52-1
Tricaine	Sigma	886-86-2
SCH79797 dihydrochloride	MCE	HY-14994
BM Purple AP	Roche	11442074001
RNA from yeast	Roche	10109223001
Proteinase K	MERCK	39450-01-6
Recombinant human VEGF-C (Cys156Ser) protein	R&D Systems	Cat# 752-VC-025
Critical commercial assays		
Tol2 kit	(Kwan et al., 2007)	N/A
LR Clonase II Plus Enzyme mix	Invitrogen	12538200
HiScribe T7 ARCA mRNA kit	NEB	#E2065S
DIG RNA Labeling Mix	Roche	11277073910
TB Green Fast RT-PCR Mix	TAKARA	RR430A
Experimental models: Cell lines		
Human Primary Lymphatic Endothelial Cells	CellBiologics	H-6092
Experimental models: Organisms/strains		
Zebrafish: Tg(fli1a:EGFP)^{y1}	(Jin, 2005)	N/A
Zebrafish: Tg(fli1aep:DsRedEX)^{um13}	(Proulx et al., 2010)	N/A
Zebrafish: Tg(fli1a:nEGFP)^{y7}	(Roman et al., 2002)	N/A
Zebrafish: Tg(kdrl:mCherry)	(Proulx et al., 2010)	N/A
Zebrafish: Tg(lyve1b:TopazYFP)^{tsu}	This paper	N/A
Oligonucleotides		
sgRNA targeting sequence: par1 : GGGGGAAGCGGCTTTAGTTCGGG	This paper	N/A

(*Continued on next page*)

Continued

REAGENT or RESOURCE	SOURCE	IDENTIFIER
sgRNA targeting sequence: gnai2a: GTGCAAGCAGTATCGAGCTG	This paper	N/A
sgRNA targeting sequence: mmp13b: CCTCCTGGAATCGGCATTGG	This paper	N/A
siRNA targeting sequence: PAR1: UAGAGUGUGAUGUAUGUGUAA	This paper	N/A
siRNA targeting sequence: GNA11: CAGUGAUACUUGUAUAUUACA	This paper	N/A
siRNA targeting sequence: GNA13: GGUGGUCAGAGAUCAGAAAGG	This paper	N/A
siRNA targeting sequence:GNAI2: CCUUGAGCGCCUAUGACUUTT	This paper	N/A
siRNA targeting sequence:MMP1: GCGUGUGACAGUAAGCUAACC	This paper	N/A
Morpholino: MO-par1 CCGTCACCAACAGAACCCGCAACAT	Gene Tools	N/A
Morpholino: MO-gnai2a GCTTCAGGGCGACGGATTTATGA	Gene Tools	N/A
Morpholino: MO-gna11a TCCAGAGTCATCACCACAGCGTTTG	Gene Tools	N/A
Morpholino: MO-gna11b GACTCTAAAGTCATCCCCACTGCTT	Gene Tools	N/A
Morpholino: MO-gna13a AAATCCGCCATCTTTGTAGTAGCGA	Gene Tools	N/A
Morpholino: MO-gna13b AGGAAATACGCCATCTTTGTGCAAC	Gene Tools	N/A
Morpholino: MO-F2 GCTGCAAGCCTCGGACGTGCGCCAT	Gene Tools	N/A
Probe for WISH, see Table S1	This paper	N/A
Primers for XX, see Table S1	This paper	N/A
Software and algorithms		
Prism	GraphPad	7.0e

RESOURCE AVAILABILITY

Lead contact

Further information and requests for resources and reagents should be directed to the lead contact: Yeqi Wang (yeqi.wang@cqu.edu.cn).

Materials availability

Transgenic zebrafish lines and mutants generated in this study are available from lead contact upon request.

Data and code availability

Any additional information required to reanalyze the data reported in this paper is available from the lead contact upon request. This paper does not report original code.

EXPERIMENTAL MODEL AND SUBJECT DETAILS

Zebrafish

Zebrafish (*Danio rerio*) embryos were incubated in Holtfreter's solution at 28.5°C(Wang et al., 2011). The following transgenic fish lines were used: *Tg(fli1a:EGFP)*^{y1} (ref. (Jin, 2005)), *Tg(fli1aep:DsRedEX)*^{um13} (ref.

(Proulx et al., 2010)), *Tg(fli1a:nEGFP)*^{y7} (ref. (Roman et al., 2002)), *Tg(kdrl:mCherry)* (ref. (Proulx et al., 2010)), and *Tg(lyve1b:TopazYFP)*^{tsu} (ref. [34]), which were gifted by Prof. Anming Meng from Tsinghua University, China, and were generated according to a previous report (Okuda et al., 2012). All zebrafish maintenance and experiments were carried out in accordance with the guidelines approved by the Ethics Committee of Chongqing University.

METHOD DETAILS

Generation of the zebrafish transgenic line

To generate the construct for *Tg(lyve1:mCherry)* and *Tg(lyve1:cleaved-par1-P2A-mCherry)*, we used Gateway-compatible vectors of the Tol2kit (Kwan et al., 2007). For venous and lymphatic expression, a 5.2 kb fragment of the zebrafish *lyve1* promoter (Okuda et al., 2012) was subcloned into p5E-MCS. Zebrafish *par1* cDNA, which lacks 87 bp within its N-terminal, was amplified by PCR. Then this *par1* fragment, P2A sequence, and mCherry sequence were subcloned into pME-cleaved-par1-P2A-mCherry plasmid. The p5E-lyvel1 plasmid was combined with pME-mCherry or pME-cleaved-par1-P2A-mCherry, the 3′ entry clone p3E-polyA, and the pDestTol2pA2 destination vector to create the pDest-lyve1:mCherry or pDest-lyve1:cleaved-par1-P2A-mCherry construct using LR Clonase II Plus Enzyme mix (Invitrogen, Cat#12538200). Embryos in the one-cell stage were injected with 25 ng/μL plasmid and 25 ng/μL Tol2 transposase RNA. Embryos injected with pTol2-lyve1:mCherry or pTol2-lyve1:cleaved-par1-P2A-mCherry were raised to adults and screened for founders.

Generation of zebrafish mutants using CRISPR/Cas9 technology

Zebrafish mutants were generated using CRISPR/Cas9 from Nanjing XinJia Medical Technology, Co., LTD, China. Briefly, the *par1* zebrafish mutant was targeted to exon 2 of the *par1* gene locus, with the target sequence 5′- GGGGGAAGCGGCTTTAGTTCGGG -3′; the *gnai2a* zebrafish mutant was targeted to exon 3 of the *gnai2a* gene locus, with the target sequence 5′-GTGCAAGCAGTATCGAGCTG-3′; and the *mmp13b* zebrafish mutant was targeted to exon 4 of the *mmp13b* gene locus, with the target sequence 5′-CCTCCTGGAATCGGCATTGG-3′. Cas9 mRNA (600 ng/μL) and *par1*, *gnai2a*, and *mmp13b* gRNA (300 ng/μL) were co-injected into wild-type embryos in the one-cell stage. Founder (F_0) were grown into adulthood and then were identified by genomic PCR and sequencing. Next, to confirm germline-transmitted mutations of *par1*, *gnai2a*, and *mmp13b*, the identified F_0 were crossed with wildtype fish to obtain heterozygous mutant zebrafish (F_1). These were in-crossed to generate homozygous mutant embryos (F_2) and used for the experimental analyses. Genotyping was carried out to distinguish between siblings (wild type), heterozygous mutants, and homozygous mutants after PCR amplification of target sites using caudal fin DNA (for adulthood) or whole embryo DNA (for embryonic stage); sequencing was used for verification. The primers for genotyping *par1* zebrafish mutant, *gnai2a* zebrafish mutant, and *mmp13b* zebrafish mutant are listed in Table S1.

Microinjection of MOs

All MOs were ordered from Gene Tools LIC. Embryos in the one-cell stage were injected with 4 ng antisense MO/embryo. TD formation of embryos at 5 dpf was observed by via confocal microscopy (Leica, SP8, Germany). The MO sequences used are listed in key resources table.

Antagonist exposure

A stock solution of SCH79797 was dissolved in DMSO to 10 mM, and a working solution was freshly prepared by diluting the stock solution to 100 nM with E3 embryo medium (5 mM NaCl, 0.17 mM KCl, 0.33 mM $CaCl_2$, and 0.33 mM $MgSO_4$). Then 100 *Tg(fli1a:EGFP)* zebrafish embryos were collected and equally divided into two groups at random. One group was exposed to the SCH79797 working solution, and the other group was exposed to vehicle control. The solutions were used to treat embryos at 1 dpf and were changed once a day; dead embryos were removed using a stereoscopic microscope (Carl Zeiss, Jena, Germany). TD formation of zebrafish embryos at 5 dpf in both groups was observed via confocal microscopy (Leica, SP8, Germany).

Imaging

Zebrafish embryos were treated with 0.003% 1-phenyl-2-thiourea (PTU, Sigma) to prevent pigment formation from 24 hpf. And the embryos were mounted in 0.8% low-melting agarose (Sigma) from imaging. For

imaging, Leica SP8 microscopy was setting as following: magnification 25× water objective, 0.75× zoom in, and a step size of 1.5 μm.

In situ hybridization

WISH of zebrafish embryos was following the standard procedure. Stained embryos were mounted in 5% methylcellulose and glycerol, and the images were captured unsing a microscope (ZEISS Stemi 2000-C) (Li et al., 2012). The probe primers of specific genes are listed in Table S1.

Whole mount immunostaining

Live embryos were fixed in fresh 4% paraformaldehyde at 4°C overnight. The embryos were washed three times and dehydrated through a series of washings with methanol in PBST. Then they were placed in 100% methanol at -20°C overnight and re-dehydrated through a series of washings with methanol in PBST. The samples were gradually warmed in Tris buffer (150 mM Tris-HCl, pH 9.0), placed in a water bath from 37°C to 70°C, and then kept for 30 min. This was followed by gradually cooling to room temperature. Then the embryos were treated with Proteinase K (30 μg/mL) for 40 min for Prox1 staining or with Proteinase K (10 μg/mL) for 5 min for p-Erk1/2 staining at room temperature. Next, we blocked the embryos for 3–4 h at 4°C and then incubated them with the primary antibody (anti-Prox1 antibody, GeneTex: GTX128354; p-Erk1/2 antibody, Cell Signaling Technology: #4370) in 1:500 dilution buffer at 4°C overnight. The embryos were washed and then incubated with goat anti-rabbit IgG (H+L) secondary antibody (Alexa 555-1:750 dilution in dilution buffer) for 1.5 h at room temperature under dark conditions. Finally, the embryos were washed in PBST-S and PBST at room temperature before being used for imaging.

Cell culture and western blotting

Human Primary Lymphatic Endothelial Cells (HDLECs) were obtained from CellBiologicsand cultured with endothelial cell medium (ECM) and 10% fetal calf serum (FBS). All siRNAs and antibodies used in this study are listed in key resource table. Recombinant human VEGF-C (Cys156Ser) protein was purchased from R&D Systems (Catalogue: 752-VC-025). HDLECs were growth to 60-80% confluence and transfected with siRNA using RNAiMAX (Invitrogen). 72 hours after transfection, the HDLECs were serum starved for 8 hours, followed by 100 ng/ml VEGF-C stimulation. Then the HDLECs were harvested for Western blotted with standard protocol (Cui et al., 2014).

Quantitative RT-PCR analysis

Quantitative real-time PCR (qPCR) was performed with TB Green Fast RT-PCR Mix (TAKARA, RR430A). The qPCR primers are listed in Table S1.

QUANTIFICATION AND STATISTICAL ANALYSIS

We used 6 somites/embryo, 6 somites/embryo, 8 ISVs/embryo, 7 somites/embryo, 7 somites/embryo, and 8 somites/embryo to quantify TD formation, LECs nuclear number, lympho-venous sprouting in the PCV, PL sprouting, Prox1 expression staining, and p-Erk1/2 expression staining in the PCV, respectively. All statistical analyses were done using GraphPad Prism software. The statistical significance of the difference between control and experimental groups was determined using the Student's unpaired two-tailed t-test followed by one-way analysis of variance. Data are presented as mean ± SEM. *P*-values ≤ 0.05 were considered significant. ***<0.0001, **<0.001, *<0.01, ns>0.01.